

# Environmental stability of highly conductive nominally undoped ZnO layers

Matej Hálal<sup>1</sup>, Yukari Inoue<sup>2</sup>, Hiroki Kato<sup>2</sup>, Germain Rey<sup>1</sup>, Florian Werner<sup>1</sup>, Christian Schubbert<sup>3</sup>, Michael Algasinger<sup>3</sup>, Thomas Dalibor<sup>3</sup>, Susanne Siebentritt<sup>1</sup>

<sup>1)</sup> Laboratory for Photovoltaics, Physics and Materials Science Research Unit, Université du Luxembourg, 41, rue du Brill, L-4422 Belvaux, Luxembourg

<sup>2)</sup> TDK Corporation Technical Center, 2-15-7, Higashi Owada, Ichikawa, Chiba, 272-8558 Japan

<sup>3)</sup> AVANCIS GmbH, Otto-Hahn-Ring 6, 81739 München, Germany

**Abstract**—Highly conductive nominally undoped ZnO (b-ZnO) films represent an attractive alternative for ZnO:Al windows employed in thin film solar cells. In order to assess their suitability for the PV industry, we examine here their stability in various environments. We show that the b-ZnO films can exhibit comparable stability to ZnO:Al films in both ambient and heated air. However, b-ZnO films degrade faster in accelerated open damp heat (DH) conditions, which can be related to their columnar microstructure. Finally, a b-ZnO multilayer coating with an improved environmental stability is presented.

**Index Terms**—TCO, zinc oxide, thin film solar cells, optoelectrical properties, stability, damp heat

## I. INTRODUCTION

In our recent work [1] we reported on preparation and characteristics of highly conductive ZnO layers ( $\rho \leq 1 \cdot 10^{-3} \Omega \text{cm}$ ) prepared from nominally undoped ZnO target under the condition of a low-power radio frequency (RF) substrate biasing. These layers, labelled as b-ZnO films, exhibit 2.5 times lower charge carrier density in comparison to commonly-employed ZnO:Al (AZO) films of identical resistivity. In consequence, their transparency in near infrared (NIR) spectral region is significantly improved. Furthermore, a replacement of AZO by b-ZnO as an n-doped window of various chalcopyrite and kesterites thin film solar cells was shown to enhance short-circuit current [1].

In this work we focus on the stability of the b-ZnO films that is tested using ageing in various environments. These include ambient air, heated air at 105°C, as well as the accelerated ageing in open damp heat (DH) using 95°C and 85% humidity. Finally, we discuss a novel multilayered b-ZnO coating that possesses an improved environmental stability.

## II. RESULTS AND DISCUSSION

### A. Ambient Air Ageing

The ambient stability of b-ZnO films deposited on flat soda lime glass (SLG) substrates was investigated by monitoring their resistivity,  $\rho$ , during a long period of ambient air exposure (i.e., room conditions), and compared to that of a reference AZO film.

Figure 1(a) depicts that the resistivity of the AZO films does not change significantly (increases by less than 2 % during 24 months of air exposure). Instead, the resistivity of the b-ZnO films of various thickness (280 - 520 nm) analysed during the

same period of time slightly increases, by 4 % (b-ZnO 420 nm) to 16 %. Even thinner b-ZnO films (than the ones presented here) that were exposed to ambient air during 32 months exhibited a resistivity rise by only 17 % (265 nm) and 24 % (255 nm), respectively ( $\Delta\rho \leq +0.3 \cdot 10^{-3} \Omega \text{cm}$ , not shown). The above observations reveal good ambient air stability of all the (unencapsulated) b-ZnO layers under investigation; it is to be stressed that such a small increase in film resistivity would not affect thin film solar cell performance.

In Fig. 1(a) it can be seen that an occasional drop in b-ZnO film resistivity that further lowers the corresponding  $\Delta\rho$  is observed. The reason for this unexpected behaviour is not yet understood, as the previously assumed correlation with the season of the year [1] was not confirmed. However, one can speculate that the actual air humidity during the resistivity analyses may be of importance since the drop in  $\Delta\rho$  is higher for thinner or more degraded samples that can exhibit a rougher surface; this effect is also witnessed by the pronounced drop in  $\rho$  of the ZnO 520 nm film after 22 months of annealing, as visible in Fig. 1(b).

### B. Dry Heat Ageing

In the second set of experiments the resistivity of b-ZnO and reference AZO films on the SLG substrates was monitored during their annealing in an oven filled with air at 105°C. The humidity within the oven was not controlled. However, it can be assumed that the water vapors can not condensate at and then penetrate within the exposed layers as this temperature is higher than boiling point. Therefore, the water-related material deterioration (discussed in section II-C) is not expected to take place and we label this test as dry heat ageing. It is to be stressed that the resistivity was analysed at the ambient temperature.

1) *The effect of b-ZnO film thickness:* The resistivity of thin b-ZnO films (thickness below 400 nm) was found to rise exponentially as depicted by blue-filled marks in Fig. 1(b) and Fig. 2(a). A steeper resistivity rise indicates an increasing rate of heat-induced degradation with decreasing film thickness. In order to understand the reason for this relation, X-Ray diffractometry (XRD) analyses have been performed on the b-ZnO layers under investigation, using the samples that were aged in the ambient air.

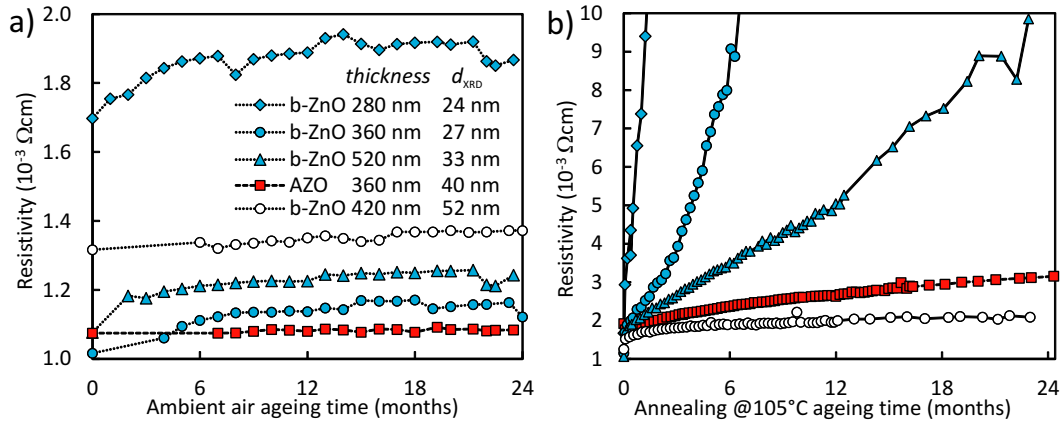


Fig. 1. Film resistivity as a function of time during 24 months of exposure to either the ambient air (a), or to the air kept at 105°C (b) for b-ZnO layers of various thickness (circle marks) and for a reference AZO layer (square marks). Film's thicknesses and XRD coherence lengths are depicted within (a).

The broadening of the ZnO (002) diffraction peak obtained in  $\theta - 2\theta$  geometry suggested that the thinner b-ZnO films possess a lower X-Ray coherence length,  $d_{\text{XRD}}$ , enumerated using the Scherrer formula [2] (depicted in the legend of Fig. 1(a)). Similar observations of smaller  $d_{\text{XRD}}$  (and a higher in-plane mechanical stress) with decreasing layer thickness were previously reported also for both ZnO and AZO [3]. A lower  $d_{\text{XRD}}$  indicates a smaller average distance between structural defects in the perpendicular direction to the substrate surface. In addition, it was found that the thinner b-ZnO films exhibit a larger broadening of the ZnO (002) diffraction peaks from rocking curve (RC) XRD analyses, suggesting a lower order of grain alignment (results not shown).

The above findings are of no surprise since the columnar structure of ZnO possess significantly smaller crystallographic features (e.g., smaller grain size and columnar width) and a lower texture degree closer to the underlying substrate as a consequence of limited growth dynamics at temperatures far from thermal equilibrium [4], [5]. In consequence, thinner films are expected to feature a higher amount of lattice defects such as open columnar boundaries also at the layer's surface. These crystalline imperfections represent possible pathways to any air-carried reactive agents (e.g.,  $\text{CO}_2$ ) that may diffuse into the film, facilitated by the elevated temperature, get adsorbed at the grain boundaries (e.g. in a form of carbonates), and negatively affect charge carrier transport within.

2) *Highly stable b-ZnO film due to improved crystallinity:* The relation of the film crystallinity and the dry heat ageing stability is also supported by the characteristics of the 420 nm thick b-ZnO film highlighted by empty circles in Fig. 1(b). It is to be noted that the resistance of this b-ZnO film was found to rise slower (by only  $\Delta\rho \approx +0.9 \cdot 10^{-3} \Omega \text{cm}$  after 24 months of annealing) than that of the 100 nm thicker b-ZnO film, and even slower than that of the reference AZO layer of similar thickness (AZO 360 nm). The same b-ZnO 420 nm film also exhibits the best ambient air stability from all the b-ZnO films, as witnessed by the lowest resistivity rise during 2 years-long ageing (Fig. 1(a)).

The  $\theta - 2\theta$  XRD analyses performed on this b-ZnO 420 nm film revealed that the ZnO (002) diffraction peak possesses a significantly higher intensity than observed from any other b-ZnO film prepared in our laboratory, indicating an enhanced crystallinity. The other XRD characteristics do also suggest such conclusion (results not shown);  $d_{\text{XRD}}$  is substantially larger (52 nm), and the broadening of the RC ZnO (002) diffraction peak is significantly smaller ( $4.1^\circ$ ), than are the respective values obtained from other four reference b-ZnO films of 370 – 400 nm thickness (26 – 30 nm and  $7.7 - 9.7^\circ$ ), and from three reference AZO films of 370 – 390 nm thickness (38 – 44 nm, and  $7.0 - 9.7^\circ$ ). It can thus be concluded that this particular b-ZnO 420 nm film has a substantially improved crystallinity compared to the other b-ZnO films under investigation and also to the AZO films of comparable thickness. A lower amount of structural imperfections may then hinder the penetration of air-carried reactive substances into the film, and thus improve its stability.

Based on the environmental tests depicted in Fig. 1 and on the presented results of the crystallographic analyses, it can be stated that the b-ZnO films prepared under the optimized deposition conditions can exhibit comparable ambient and heat stability as the standard AZO films. However, these conditions are yet to be defined.

3) *Electrical and structural changes due to dry annealing:* In order to get an insight into the degradation mechanism of b-ZnO films, the resistivity of a 250 nm thick film was monitored during 5 600 hours of annealing, and consequently during another 15 400 hours of ambient air ageing. Afterwards, it was characterized by Hall and XRD analyses.

Fig. 2(a) depicts that the film resistivity rose by four orders of magnitude in consequence of the dry heat ageing, and that a partial recovery by one order of magnitude is observed once the annealed film is removed from the oven. The resistivity increase can be attributed to both loss of electron density,  $n_e$ , and to the lower electron mobility,  $\mu_e$ . The Hall analyses (summarized in Fig. 2(b)) revealed that  $n_e$  of this dry annealed film has dropped 11 times and  $\mu_e$  even 26 times if compared

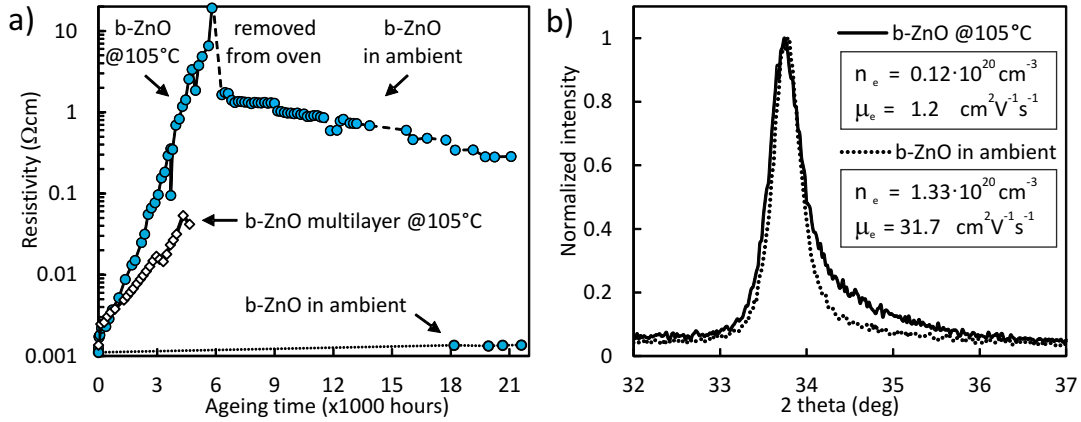


Fig. 2. (a) The evolution of the film resistivity of 250 nm thick b-ZnO film that was first aged in air at 105°C for 5 600 hours, and then removed to the ambient air (filled marks and solid line). The resistivity of the reference piece of the same b-ZnO 250 nm film left in the ambient air (filled marks and dotted line) and of another b-ZnO 250 nm film covered by a 70 nm thick b-ZnO overlayer (b-ZnO multilayer) and aged by dry annealing (empty marks) are also shown. (b)  $\theta - 2\theta$  XRD diffractograms with ZnO (002) peak of the b-ZnO 250 nm film that was either aged by dry annealing (solid line) or left in the ambient air (dotted line), analysed after approx. 18 000 hours (24 months) since fabrication. The corresponding electron density and Hall mobility values are in the inset.

to  $n_e$  and  $\mu_e$  of the reference piece of the identical film that was prepared in the same deposition process and left in the ambient air for more than 29 months (for which  $\Delta\rho < +0.3 \cdot 10^{-3} \Omega\text{cm}$ , as also depicted in Fig. 2(a)).

Fig. 2(b) depicts the normalized  $\theta - 2\theta$  XRD diffractograms obtained from the two pieces of the b-ZnO 250 nm film after 24 months since their deposition. It can be seen that the ZnO (002) diffraction peak of the b-ZnO films that was aged by dry annealing exhibits a significantly wider shoulder at the higher diffraction angles. This shoulder suggests a variation in the  $c$  lattice parameter; the higher the angle is, the smaller the  $c$  value (closer to its unstrained value) should be.

This assumption was verified by grazing incidence (GI) analyses performed at various angles, which in all cases revealed a larger high-angle shoulder of the ZnO (002) diffraction peak obtained from the dry annealed b-ZnO (results not shown). Moreover, the GI analyses indicated that the suggested variation in  $c$  takes place at the film surface, as the area enclosed by the high-angle shoulders of the GI diffractograms from the dry annealed piece and from the other one kept in ambient air increased by a factor of 2 if the GI angle was lowered from 0.4 degrees (higher XRD penetration depth) to 0.3 degrees (lower XRD penetration depth). It is to be noted that the latter angle lies in the proximity of the X-ray critical angle, as suggested by an order-of-magnitude lower ZnO (002) diffraction peak intensity (not shown), and as predicted by a substantial drop in the XRD attenuation length in ZnO evaluated numerically.

The above observations imply the existence of a modified near-surface region with a lower lattice strain, as the  $c$  of the annealed b-ZnO film is smaller closer to the exposed surface. It is thus evident that the deterioration of charge carrier characteristics of thin b-ZnO films can be related to the structural changes in consequence of the dry heat ageing.

### C. Open Damp Heat Ageing

Accelerated ageing in open DH conditions during a week period was performed on the two representatives of the standard i-layer/n-layer stacks used as a front contact of chalcopyrite and kesterite solar cells. In these experiments, the ZnO/b-ZnO and ZnO/AZO bilayers (80 nm/360 nm in thickness) were prepared onto bare SLG substrates, characterised for the optoelectrical properties, and then submitted to the environmental chamber using 95°C and 85 % relative humidity. It is to be stressed that neither of the coatings was moisture-protected by any kind of foil-glass or glass-glass laminate, resulting in a much harsher test condition as compared to the standard environmental test IEC 61646. The coatings were regularly removed from the DH chamber after selected numbers of hours for the purpose of resistivity and Hall analyses, and the respective results are shown in Fig. 3.

One should note that prior to DH ageing the examined b-ZnO film exhibits about 2.3 times higher electron mobility and about 2.6 times lower electron density in comparison to the AZO film (at 0 hours in Fig. 3(b) and (c), respectively). It is due to its lower free electron density that the b-ZnO film shows a significantly higher transmittance and a lower reflectance in the NIR region (Fig. 3(d)).

Fig. 3(a) illustrates that a week-long accelerated DH ageing causes a four-fold increase in b-ZnO film resistivity, in contrast to the AZO film for which much lower rise is observed (by 65 %). The increase in  $\rho$  in both cases can be related mostly to the substantial decrease in Hall mobility that drops by about -70 % for the b-ZnO film and by -30 % for the AZO film (Fig. 3(b)). The electron density itself also decreases, by -30 % and by -12 %, respectively (Fig. 3(c)). Fig. 3(d) shows that there are no changes in films' transmission in the visible region. However, a pronounced rise in the NIR transparency of ZnO/b-ZnO reflects the reduced carrier density in b-ZnO.

The observed deterioration of Hall mobility, specifically

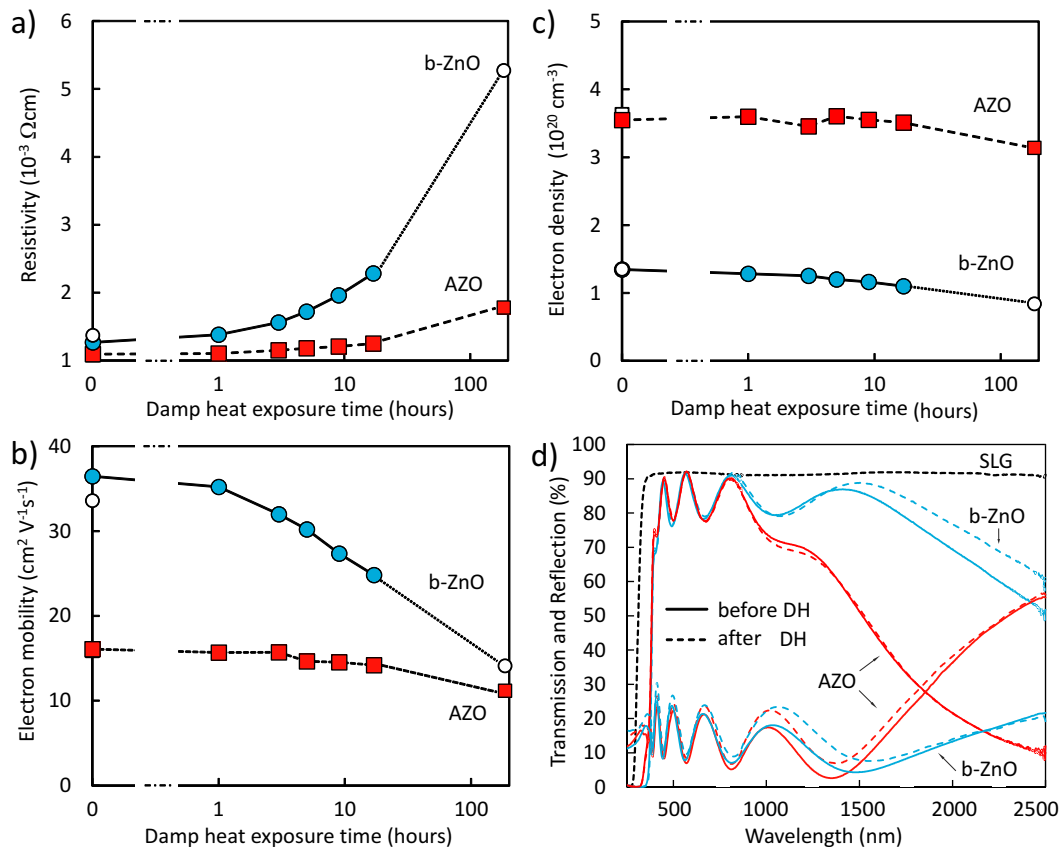


Fig. 3. The evolution of film resistivity (a), electron Hall mobility (b), and electron density (c) of ZnO/b-ZnO (circle marks) and ZnO/AZO (square marks) bilayer films, as a function of accelerated open DH exposure (in log scale). Optical transmission (higher curves) and reflection (lower curves) spectra of the two bilayers evaluated before (in solid lines) and after (in dashed lines) a week of accelerated ageing in open DH conditions are plotted in (d). The empty symbols stand for the Hall analyses performed at the University of Luxembourg and the filled symbols for those performed at AVANCIS.

pronounced for the ZnO/b-ZnO coating, suggests electronic changes caused by water vapors that can get adsorbed at the exposed film surface and/or diffuse within the film through accessible columnar and grain boundaries [6], [7], [8]. It is known that the adsorbed water molecules and their products (e.g., formed hydroxides) act as electron traps. The resulting trapped electron accumulation at the grain boundaries then raises the potential barrier that the free electrons have to overcome [9]. The increased scattering at the grain boundaries is thus the most probable reason for the observed drop in Hall mobility.

Since the density of the crystallographic imperfections that represents the accessible pathways for in-diffusion is typically higher in the b-ZnO films in comparison with the AZO films (as suggested by the lower XRD coherence length of the non-optimised b-ZnO films discussed in the previous section), the grain boundary degradation and the consequent rise in electron scattering is also expected higher within the b-ZnO films.

#### D. Multilayered b-ZnO films

In an attempt to improve the environmental stability of the b-ZnO films several multilayered b-ZnO coatings that would slow down the in-diffusion of reactive substances were

investigated. In these fabrication experiments a standard b-ZnO film was covered by a thin overlayer comprising of b-ZnO prepared at modified deposition conditions detailed elsewhere [10].

An example of such coating is the b-ZnO 250 nm film covered by a 70 nm thick b-ZnO overlayer, which was also aged in the dry heat conditions as depicted in Fig. 2(a). It can be seen that the resistivity of this "b-ZnO multilayer" monitored for more than 4 500 hours rises at a substantially lower pace than its single-layer b-ZnO counterpart. This observation suggests that the upper b-ZnO film serves as a mechanical barrier that may effectively cover some of the open columnar boundaries and other crystallographic imperfections at the surface of the underlying b-ZnO film, imposing thus a more complex path (in terms of in-diffusion) for detrimental agents.

The above assumption is further supported by the open DH experiments performed with the complete unencapsulated solar cell stacks equipped with either an AZO layer, a b-ZnO layer, or with a b-ZnO multilayer (featuring an identical 70 nm thick overlayer as the coating presented in Fig.2(a)). As the three ZnO-based layers of comparable total thickness ( $\approx 850 \text{ nm}$ ) form the front transparent contact that has the crucial function for both incoming irradiation transmission and charge carrier

transfer towards external contacts, the optoelectrical performance of the entire solar cell stack can be directly related to the environmental stability of these uppermost layers.

In the respective experiments, it was found that the solar cells equipped with the multilayered b-ZnO stack exhibit a much slower deterioration of the investigated optoelectrical characteristics than the solar cells coated with a single layer b-ZnO film [11]. For instance, the power conversion efficiency, Eff, of the solar cells equipped with b-ZnO multilayer drops in average by  $-75\%$  after 57 hours of open DH treatment. In contrast, the equally treated solar cells with a single-layer b-ZnO film exhibit an average Eff drop  $\Delta\text{Eff} = -93\%$ . (The reference solar cell featuring a standard AZO layer showed  $\Delta\text{Eff} = -51\%$ .)

### III. CONCLUSION

This work demonstrates that the highly conductive and transparent b-ZnO films are stable in the ambient air as well as in the heated air over the test period of 24 months. Their ambient air stability is in general comparable to that of the reference AZO film and the 420 nm thick b-ZnO film showed even better stability in dry heat ageing. However, we observe a faster degradation of the b-ZnO films, in terms of a more pronounced drop in both charge carrier density and Hall mobility, in accelerated open DH ageing.

These observations were related to the characteristics of the textured columnar microstructure of the investigated ZnO-based films. The XRD analyses have suggested that the microstructure of b-ZnO films exhibits smaller crystallographic features than that of the AZO films, indicating thus an easier (faster) in-diffusion of reactive substances that can deteriorate electron transport within. Finally, a prototype multilayered b-ZnO stack that can slow down the in-diffusion of these detrimental substances is proposed and tested.

### ACKNOWLEDGMENT

The authors wish to thank Mr. Thomas Schuler for his expert technical assistance, Dr. Susanne Schorr for her kind help with XRD attenuation length determination, Dr. Yves Flemming for his patient assistance with rocking curve XRD analyses, and LIST for the access to the XRD and profilometry equipment. The financial support of TDK Corporation within the NOTO project is gratefully acknowledged.

### REFERENCES

- [1] M. Hálá, S. Fujii, A. Redinger, Y. Inoue, G. Rey, M. Thevenin, V. Deprédurand, T. P. Weiss, T. Bertram, and S. Siebentritt, "Highly conductive ZnO films with high near infrared transparency," *Prog. Photovolt: Res. Appl.*, vol. 23, no. 11, pp. 1630–1641, 2015.
- [2] J. I. Langford and A. J. C. Wilson, "Scherrer after sixty years: A survey and some new results in the determination of crystallite size," *J. Appl. Crystallogr.*, vol. 11, no. 2, pp. 102–113, 1978.
- [3] R. Cebulla, R. Wendt, and K. Ellmer, "Al-doped zinc oxide films deposited by simultaneous rf and dc excitation of a magnetron plasma: Relationships between plasma parameters and structural and electrical film properties," *J. Appl. Phys.*, vol. 83, no. 2, pp. 1087–1095, 1998.
- [4] Y. Kajikawa, "Texture development of non-epitaxial polycrystalline ZnO films," *J. Cryst. Growth*, vol. 289, no. 1, pp. 387 – 394, 2006.
- [5] J. A. Thornton, "Influence of apparatus geometry and deposition conditions on the structure and topography of thick sputtered coatings," *J. Vac. Sci. Technol.*, vol. 11, no. 4, pp. 666–670, 1974.
- [6] D. Greiner, N. Papathanasiou, A. Pflug, F. Ruske, and R. Klenk, "Influence of damp heat on the optical and electrical properties of Al-doped zinc oxide," *Thin Solid Films*, vol. 517, no. 7, pp. 2291 – 2294, 2009.
- [7] F. J. Pern, B. To, S. H. Glick, R. Sundaramoorthy, C. DeHart, S. Glynn, C. Perkins, L. Mansfield, and T. Gessert, "Variations in damp heat-induced degradation behavior of sputtered ZnO window layer for CIGS solar cells," vol. 7773, 2010, p. 77730R–1.
- [8] J. Hüpkens, J. Owen, M. Wimmer, F. Ruske, D. Greiner, R. Klenk, U. Zastrow, and J. Hotovy, "Damp heat stable doped zinc oxide films," *Thin Solid Films*, vol. 555, no. 0, pp. 48 – 52, 2014.
- [9] J. Y. W. Seto, "The electrical properties of polycrystalline silicon films," *J. Appl. Phys.*, vol. 46, no. 12, pp. 5247–5254, 1975.
- [10] M. Hálá, P. Dale, and S. Siebentritt, "Transparent conducting film based on zinc oxide," patent application LU 93080 (filed 20.5.2016).
- [11] M. Hálá, Y. Inoue, H. Kato, G. Rey, F. Werner, M. Algasinger, Ch. Schubert, T. Dalibor, and S. Siebentritt, "Improved environmental stability of highly conductive nominally undoped ZnO layers suitable for n-type windows in thin film solar cells," submitted.